Irreversible inactivation of ISG15 by a viral leader protease enables alternative infection detection strategies

Kirby N. Swatek[a], Martina Aumayr[b,1], Jonathan N. Pruneda[a,1], Linda J. Visser[c,1], Stephen Berryman[d], Anja F. Kueck[a], Paul P. Geurink[e], Huib Ovaa[e], Frank J. M. van Kuppeveld[c], Tobias J. Tuthill[d], Tim Skern[b], and David Komander[a,2]

[a]Protein and Nucleic Acid Chemistry Division, Medical Research Council Laboratory of Molecular Biology, CB2 0QH Cambridge, United Kingdom; [b]Department of Medical Biochemistry, Max F. Perutz Laboratories, Vienna Biocenter, Medical University of Vienna, A-1030 Vienna, Austria; [c]Department of Infectious Diseases & Immunology, Virology Division, Faculty of Veterinary Medicine, Utrecht University, 3584CL Utrecht, The Netherlands; [d]The Pirbright Institute, GU24 0NF Pirbright, Surrey, United Kingdom; and [e]Department of Chemical Immunology, Leiden University Medical Centre, 2333 ZC Leiden, The Netherlands

Edited by Brenda A. Schulman, Max Planck Institute of Biochemistry, Planegg, Germany, and approved January 12, 2018 (received for review June 12, 2017)

In response to viral infection, cells mount a potent inflammatory response that relies on ISG15 and ubiquitin posttranslational modifications. Many viruses use deubiquitinases and deISGylases that reverse these modifications and antagonize host signaling processes. We here reveal that the leader protease, Lb^{pro}, from foot-and-mouth disease virus (FMDV) targets ISG15 and to a lesser extent, ubiquitin in an unprecedented manner. Unlike canonical deISGylases that hydrolyze the isopeptide linkage after the C-terminal GlyGly motif, Lb^{pro} cleaves the peptide bond preceding the GlyGly motif. Consequently, the GlyGly dipeptide remains attached to the substrate Lys, and cleaved ISG15 is rendered incompetent for reconjugation. A crystal structure of Lb^{pro} bound to an engineered ISG15 suicide probe revealed the molecular basis for ISG15 proteolysis. Importantly, anti-GlyGly antibodies, developed for ubiquitin proteomics, are able to detect Lb^{pro} cleavage products during viral infection. This opens avenues for infection detection of FMDV based on an immutable, host-derived epitope.

ubiquitin | ISG15 | viral signaling | FMDV | structure

Picornaviruses are nonenveloped, positive-strand RNA viruses that comprise small genomes but represent significant threats to human and animal health (1). For example, foot-and-mouth disease virus (FMDV) is a global, highly infectious animal pathogen that causes annual economic losses in livestock farming estimated between $6.5 and $21 billion US dollars (2). Infected cattle develop fever and vesicular lesions in their mouths and hooves; consequently, FMDV outbreaks lead to culling of entire herds in FMDV-free countries to prevent the spread of the virus (3).

Among the 14 mature proteins encoded by FMDV are two peptidase activities required for self-processing and viral proliferation (4, 5). The leader protease Lb^{pro} is a papain-like cysteine protease that has several roles (4, 6). First, Lb^{pro} cleaves its own C terminus, releasing itself from the nascent polyprotein. Second, Lb^{pro} also cleaves the two isoforms of eukaryotic initiation factor 4G (eIF4G), the inactivation of which diverts ribosomes to preferentially translate viral RNA via their internal ribosome entry site (4, 6). Third, Lb^{pro} was reported to subvert innate immune signaling pathways by acting as a deubiquitinase (DUB) (7).

Ubiquitination is a key signaling mechanism used by cells to detect and respond to viral infection (8). Various ubiquitin signals play important roles during the activation of transcriptional programs, such as the NF-κB and IFN response (8, 9). With the initiation of IFN signaling, the products of roughly 300 IFN stimulated genes (ISGs) mount an antiviral response (10). Among the ISGs are the ubiquitin-like modifier ISG15 and its assembly machinery consisting of UBE1L, UBE2L6/UbcH8, and the HECT E3 ligase HERC5 (11). ISG15 comprises two ubiquitin fold domains in tandem [an N-terminal ubiquitin-like domain (NTD) and a C-terminal ubiquitin-like domain (CTD)], and like ubiquitin, it is attached to Lys residues on target proteins via its C-terminal Gly-Gly (Gly156–Gly157) motif. Cotranslational attachment of ISG15 to viral capsid proteins inhibits virus assembly (12), and additional intra- and extracellular roles of ISG15 are also emerging (13, 14). Together, ubiquitin and ubiquitin-like modifications regulate most antiviral signaling cascades.

Viruses are well-known to counter these defenses and manipulate the regulatory machineries or the modifications themselves (8, 9, 15). For instance, Crimean Congo hemorrhagic fever virus (CCHFV), severe acute respiratory syndrome coronavirus, and Middle East respiratory syndrome coronavirus all encode proteases with dual deISGylase and DUB activity (16).

We here show that FMDV Lb^{pro} targets ISG15 with strong preference over ubiquitin and NEDD8 and characterize this specificity biochemically and structurally. We uncover a previously undescribed mechanism by which viruses interfere with the ubiquitin and ubiquitin-like systems. Unlike canonical deISGylases, Lb^{pro} does not target the isopeptide bond formed

Significance

An understanding of the mechanisms by which viruses evade host immunity is essential to the development of antiviral drugs and viral detection strategies. Ubiquitin and ubiquitin-like modifications are crucial in cellular innate immune and infection responses and are often suppressed by viral proteins. We here identify a previously unknown mechanism of viral evasion. A viral protease, Lb^{pro}, removes ubiquitin and the ubiquitin-like protein ISG15 incompletely from proteins. While this strategy efficiently and irreversibly shuts down these modification systems, it enables repurposing of tools and technologies developed for ubiquitin research in virus detection. Specifically, we show that foot-and-mouth disease virus infection can be detected using an anti-GlyGly antibody developed for ubiquitin mass spectrometry research.

Author contributions: K.N.S., L.J.V., S.B., F.J.M.v.K., T.J.T., T.S., and D.K. designed research; K.N.S., M.A., J.N.P., L.J.V., S.B., and A.F.K. performed research; P.P.G., H.O., F.J.M.v.K., and T.J.T. contributed new reagents/analytic tools; K.N.S., M.A., J.N.P., L.J.V., S.B., F.J.M.v.K., T.J.T., T.S., and D.K. analyzed data; and K.N.S. and D.K. wrote the paper.

Conflict of interest statement: D.K. is part of the DUB Alliance, which includes Cancer Research Technology and FORMA Therapeutics.

This article is a PNAS Direct Submission.

Data deposition: The crystallography, atomic coordinates, and structure factors have been deposited in the Protein Data Bank, www.wwpdb.org (PDB ID code 6FFA).

[1]M.A., J.N.P., and L.J.V. contributed equally to this work.

[2]To whom correspondence should be addressed. Email: dk@mrc-lmb.cam.ac.uk.

This article contains supporting information online at www.pnas.org/lookup/suppl/doi:10.1073/pnas.1710617115/-/DCSupplemental.

Published online February 20, 2018.

during attachment but selectively cleaves a peptide bond in the C terminus of ISG15, which results in incomplete removal of the modifier. A crystal structure of Lb^{pro} covalently bound to a specifically designed ISG15 suicide probe reveals the molecular basis of Lb^{pro} specificity and substrate promiscuity. Importantly, cleavage by Lb^{pro} exposes a GlyGly epitope on substrates of the modifier, and we show that this epitope can be detected in cells during FMDV infection with relative ease. Such mechanism- and activity-based detection strategy opens avenues for distinguishing infected from vaccinated animals and may help limit the economic impact of FMDV.

Results

Lb^{pro} Substrate Specificity and Cleavage. We used ubiquitin and ubiquitin-like model substrates (17) to characterize Lb^{pro} DUB activity in vitro (Fig. S1*A*) and surprisingly found that while the enzyme lacked robust DUB activity, it targeted ISG15 with high activity and specificity (Fig. 1*A*). Ubiquitin cleavage required 1,000-fold higher enzyme concentration (Fig. S1*B*). Kinetic analysis revealed deISGylase activity comparable with previously studied viral (18, 19) and human enzymes (20) (Fig. 1*B* and Fig. S1*C*). However, a number of standard measurements for deISGylation activity were negative. ISG15-derived suicide probes that covalently modify ISG15-reactive Cys proteases (21, 22) were unable to modify Lb^{pro} (Fig. 1*C* and Fig. S1*D*). Hydrolysis of ISG15 7-amido-4-methylcoumarin (AMC) by deISGylases, such as the viral ovarian tumor (vOTU) domain of CCHFV, leads to fluorescence, yet Lb^{pro} did not generate a fluorescent signal in this assay (Fig. S1 *E* and *F*). In contrast, slightly extended precursor forms of full-length proISG15 (amino acids 1–165; featuring an additional eight residues at the C terminus) or $proISG15^{CTD}$ (amino acids 79–165) were rapidly hydrolyzed by Lb^{pro} (Fig. 1*D*). Strikingly, mass spectrometry (MS) analysis of Lb^{pro}-treated mature $ISG15^{CTD}$ (amino acids 79–157) revealed a truncated ISG15 molecule; Lb^{pro} had cleaved ISG15 between Arg155 and the C-terminal Gly156–Gly157 sequence (Fig. 1 *E* and *F*).

This surprising result was corroborated in additional experiments. We compared the cleavage rates of pro-, mature-, and substrate-bound forms of ISG15 by intact MS analysis, revealing similar activity of Lb^{pro} against pro- and mature ISG15 and slightly higher activity toward ISG15 linked to 5-tetramethylrhodamine (TAMRA)-labeled Lys-Gly dipeptide via an isopeptide bond (Fig. S1*G*). This showed that Lb^{pro} can process all forms of ISG15 present in cells.

The cleavage site of Lb^{pro} contrasts all known deISGylases, which cleave ISG15 from substrates, such that both proteins are recycled to the same state as they were before modification (18, 19). In hindsight, these findings explain the inability of Lb^{pro} to react with the ISG15 suicide probe (in which the reactive warhead would extend beyond the active site) or generate a signal in the ISG15-AMC assay. AMC only fluoresces in the unmodified form, whereas Lb^{pro} cleavage produces a nonfluorescent GlyGly-modified AMC reagent (Fig. S2*A*).

At higher enzyme concentrations, ubiquitin and NEDD8 were also cleaved at an identical site between Arg74 and the C-terminal GlyGly motif, whereas SUMO1 was not cleaved (Fig. S2 *B–D*). Hence, Lb^{pro} removes ISG15 (as well as ubiquitin and NEDD8) in a manner that leaves a GlyGly remnant attached to a substrate

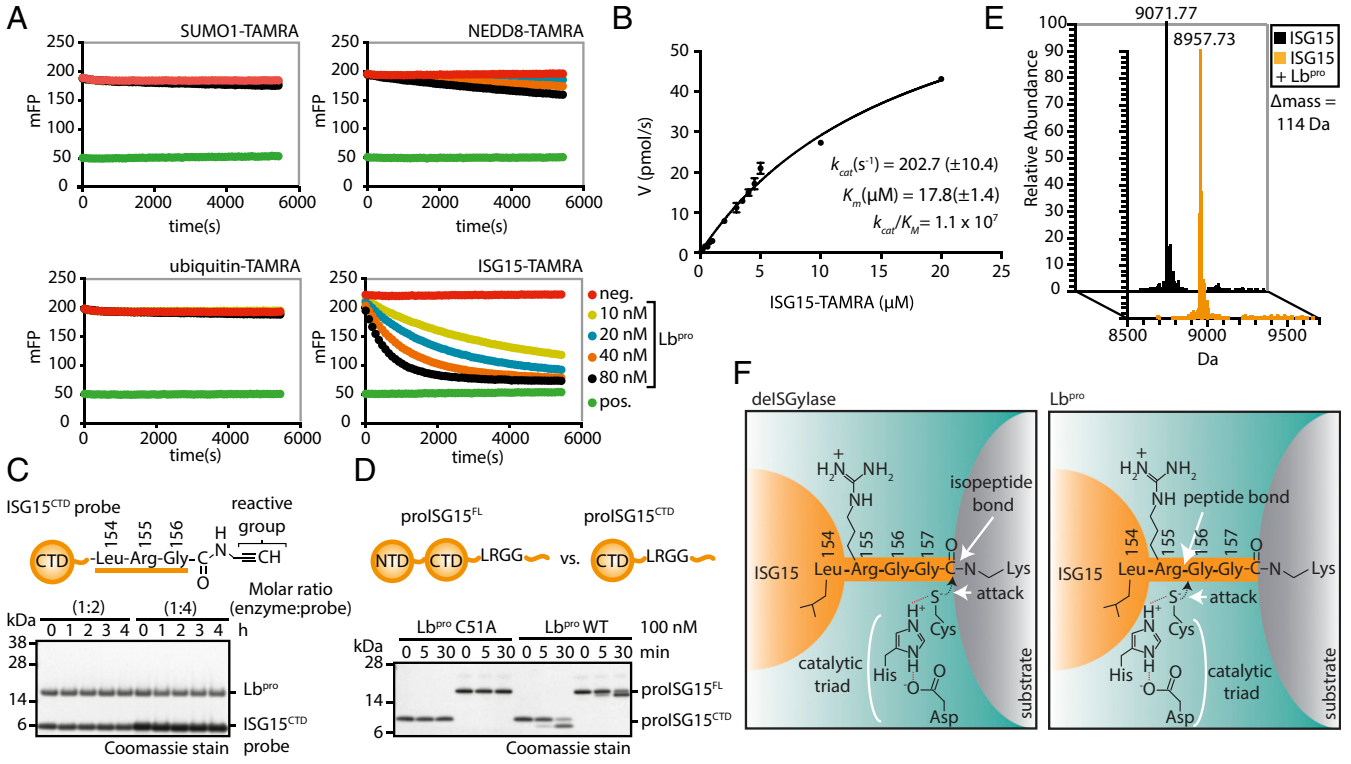

Fig. 1. Lb^{pro} substrate specificity and cleavage. (*A*) Specificity analysis of Lb^{pro} against ubiquitin and ubiquitin-like (SUMO1, NEDD8, ISG15) TAMRA substrates (Fig. S1). (*B*) Michaelis–Menten kinetics of Lb^{pro} as measured by ISG15-TAMRA cleavage. Error bars represent SD from the mean. (*C*) Suicide ISG15 probe assays were performed with Lb^{pro} and WT $ISG15^{CTD}$ probe. (*D*) Comparison of full-length proISG15 (amino acids 1–165) and $proISG15^{CTD}$ (amino acids 79–165) cleavage by Lb^{pro}. (*E*) Electrospray ionization MS of untreated and Lb^{pro}-treated mature $ISG15^{CTD}$ (amino acids 79–157). The difference in mass corresponds to loss of the Gly-Gly peptide (114 Da). (*F*) Schematic of ISG15 cleavage by a canonical deISGylase (*Left*) and Lb^{pro} (*Right*). deISGylases cleave isopeptide bonds, while Lb^{pro} cleaves the peptide bond C-terminal to Arg155, releasing a GlyGly dipeptide. All assays were performed in triplicate. NTD, N-terminal ubiquitin-like domain.

Lys residue and renders the ubiquitin/ubiquitin-like protein incompetent toward additional rounds of conjugation.

Structure of Lb^{pro} Bound to ISG15. To decipher the mechanism of this unprecedented activity, we designed an ISG15 suicide probe specific for Lb^{pro}. As mentioned, the WT ISG15 suicide probe modified several viral proteases but was too long to modify Lb^{pro} (Fig. S2*E*). Removing the GlyGly motif from ISG15^{CTD} and replacing Arg155 with a Gly-like C-terminal propargyl warhead (Fig. 2*A*) generated an ISG15^{CTD}-ΔC probe that efficiently modified Lb^{pro} (Fig. 2*B* and Fig. S2*E*). This enabled purification, crystallization, and structure determination of a covalent Lb^{pro}~ISG15^{CTD}-ΔC complex at 1.5-Å resolution (Fig. 2 *C* and *D*, Fig. S3, and Table S1). As anticipated, the ISG15^{CTD}-ΔC probe had covalently modified the catalytic Cys51 of Lb^{pro} (Fig. S3). Individually, the Lb^{pro} protease and ISG15 domains were similar to previously determined structures (18, 23) (Cα rmsds of 0.609 and 0.274 Å, respectively).

The structure revealed how proteolytic cleavage of ISG15 is achieved (Fig. 2*E* and Fig. S3). Key interactions are formed via the ISG15 C terminus and also, via a hydrophobic surface centered on ISG15 Trp123 (Fig. S3). The positively charged residues of the ISG15 C terminus, Arg153 and Arg155 (the latter mutated to Gly in the ISG15^{CTD}-ΔC probe), are cradled by an acidic groove that consists of Asp49, Glu96, and Glu147 on Lb^{pro} (Fig. S3*G*). Furthermore, ISG15 Leu154 occupies a hydrophobic pocket commonly found in papain-like enzymes. Mutation of either Leu154 or Arg155 to Ala in proISG15 strongly reduced cleavage by Lb^{pro} (Fig. S3*H*). However, these C-terminal mutations do not prevent ISG15 binding, since the ISG15^{CTD}-ΔC suicide probe that lacks Arg155 was able to modify Lb^{pro} (Fig. 2 *B* and *C*). The importance of the C terminus explains, at least in part, the observed weak cross-reactivity with ubiquitin and NEDD8, which feature identical or similar C-terminal sequences, respectively, and also, the inability of Lb^{pro} to target other modifiers, such as SUMO1, which feature more divergent C-terminal sequences (24) (Fig. S3*F*). The observed interactions closely mimic those seen in the previously determined structure

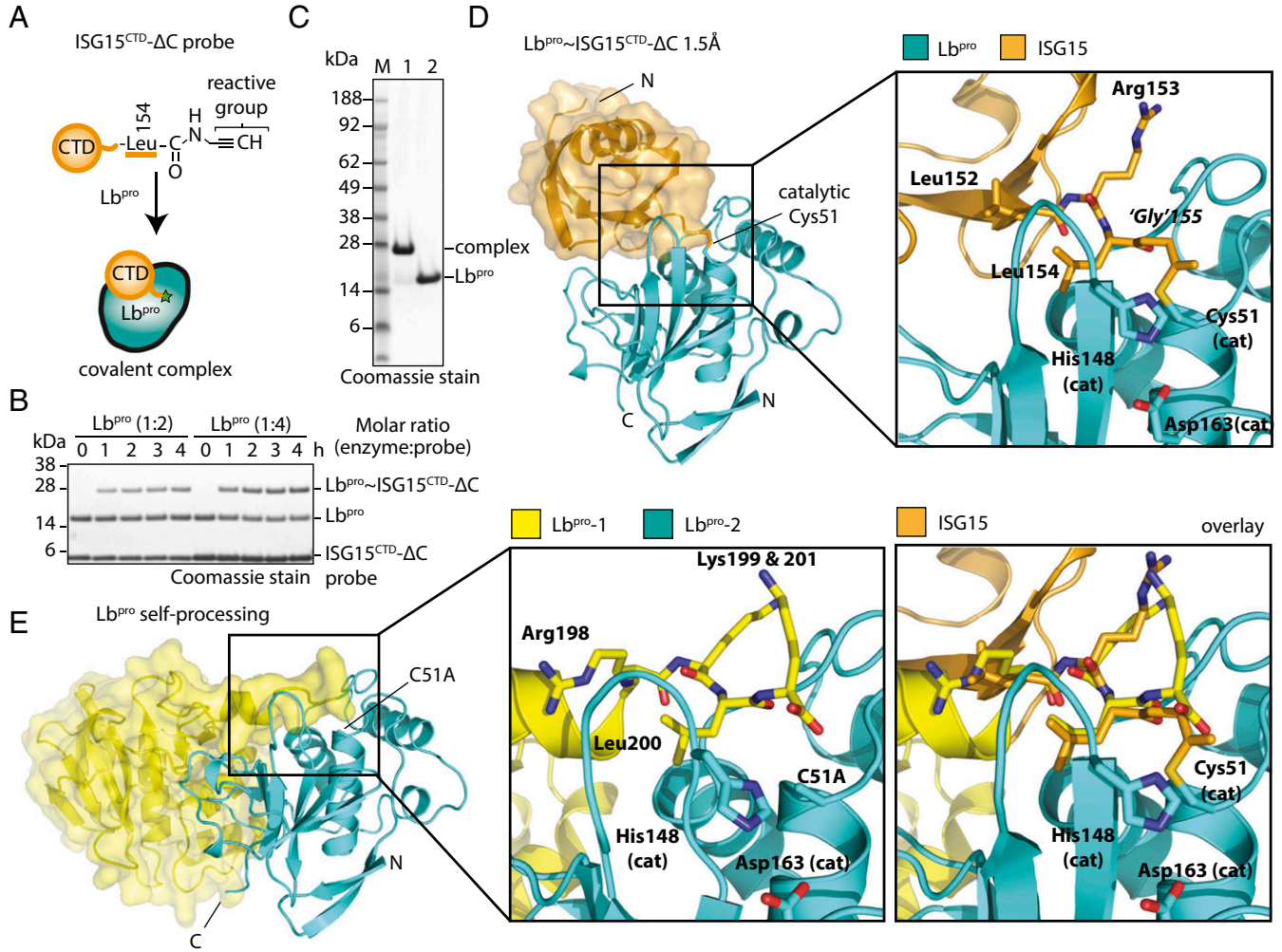

Fig. 2. Structure of Lb^{pro} bound to ISG15. (*A*) Schematic of an engineered Lb^{pro}-specific ISG15 suicide probe. (*B*) The ISG15^{CTD}-ΔC suicide probe forms a covalent complex with Lb^{pro} (indicated by ~). (*C*) SDS/PAGE of the purified Lb^{pro}~ISG15^{CTD}-ΔC complex compared with unmodified Lb^{pro}. (*D*, *Left*) Crystal structure of Lb^{pro} covalently modified with the ISG15^{CTD}-ΔC probe. (*D*, *Right*) Close-up view of the ISG15^{CTD}-ΔC modified catalytic cysteine of Lb^{pro}. The catalytic triad (Cys51, His148, Asp163) of Lb^{pro} and C-terminal residues of ISG15 (amino acids 152–154; Arg155 was replaced by the Gly-like warhead) are highlighted. (*E*, *Left*) Structure of Lb^{pro} (Protein Data Bank ID code 1qol) during self-processing in *trans*. The Lb^{pro} substrate positioned for *trans* self-processing (yellow; Lb^{pro}-1) and the catalytic Lb^{pro} (cyan; Lb^{pro}-2) are shown. (*E*, *Center*) Lb^{pro} C-terminal residues of the substrate (Lb^{pro}-1) are shown (Arg198, Lys199, Leu200, Lys201), and residues of the catalytic triad are shown as in *D* for Lb^{pro}-2. (*E*, *Right*) The Lb^{pro}~ISG15^{CTD}-ΔC and Lb^{pro} self-processing structures were overlaid. Gel-based assays in *B* were performed in triplicate.

of Lb^{pro} carrying out self-processing of its own C terminus (23) (Fig. 2*E* and Fig. S3*F*).

Analysis of ISG15 Specificity. Another interaction site between ISG15 and Lb^{pro} centers on the conserved Trp123 of ISG15 (Fig. 3*A* and Fig. S4*A*), the main hydrophobic ISG15 surface used in other deISGylases (Fig. S4*B*) (18, 19, 22, 25). Lb^{pro} utilizes a corresponding hydrophobic ISG15 binding surface formed by Leu92, Pro99 in the α3/α4 loop, and residues, including Leu102 on the α4 helix to shape the overall structure of the binding site (Fig. 3*A* and Fig. S3*C*); mutations in these residues decrease Lb^{pro} activity toward ISG15 (Fig. 3*B* and Fig. S4*C*). Importantly, this loop is not involved in interactions used during self-processing (Fig. 2*E*), and consequently and consistently, mutants in the ISG15 binding site are neither affected in their ability to self-process nor affected in their ability to cleave eIF4G (Fig. S5). Hence, substrate and ISG15 binding sites are spatially separated.

In ISG15, mutation of Trp123 to Ala leads to a significant reduction of cleavage by Lb^{pro} (Fig. 3*C*). Trp123 is also a major difference between ISG15 and ubiquitin, where the structurally equivalent residue is Arg42 (Fig. 3*D*). Mutation of ubiquitin Arg42 to Trp in the context of an Met1-linked ubiquitin chain significantly reduced cleavage of this chain type by the Met1 linkage-specific DUB OTULIN (26) (Fig. S4*D*) but enhanced ubiquitin chain cleavage by Lb^{pro} (Fig. 3*E* and Fig. S4*E*). This reveals one component of how Lb^{pro} distinguishes modifiers.

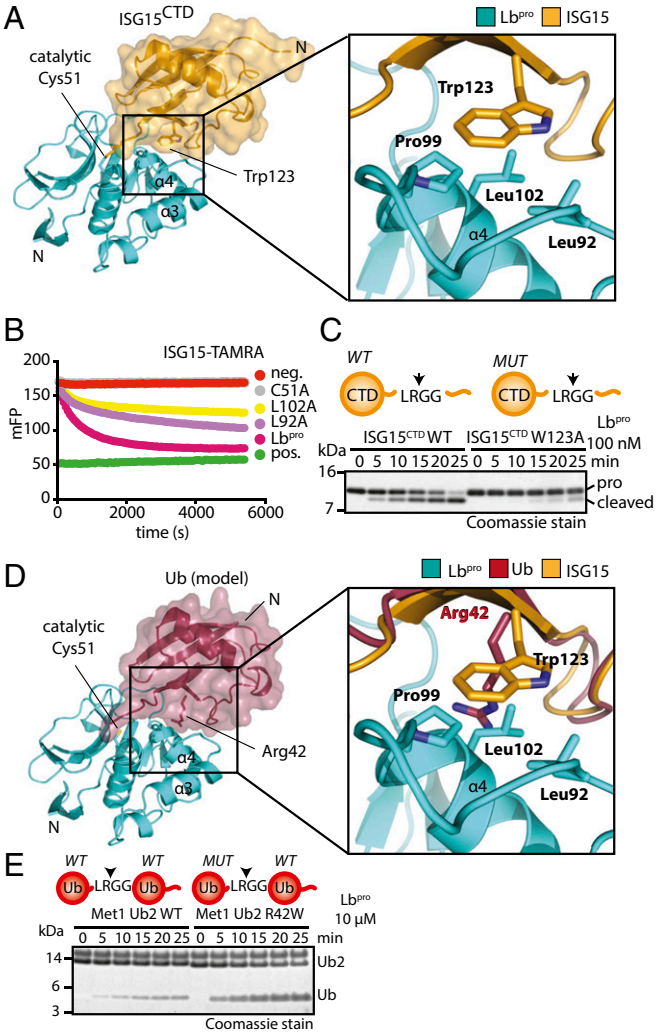

Fig. 3. Structural analysis of ISG15 specificity. (*A*, *Left*) The Lb^{pro}~ISG15^{CTD}-ΔC complex is shown as in Fig. 2*D*. (*A*, *Right*) Close-up view of the hydrophobic contact between Lb^{pro} (Leu92, Pro99, Leu102) and ISG15 (Trp123) (Fig. S4). (*B*) ISG15-TAMRA cleavage assays with Lb^{pro} point mutants in the hydrophobic patch. (*C*) Lb^{pro} cleavage assays with WT and W123A proISG15^{CTD}. (*D*, *Left*) Model of ubiquitin (Protein Data Bank ID code 1ubq) bound to Lb^{pro}. Ubiquitin (red) was superimposed onto ISG15^{CTD}. (*D*, *Right*) Close-up view of the analogous interface as in *A*. (*E*) Met1 diubiquitin cleavage assays with or without R42W mutation in the distal ubiquitin. Arrows in the schematics show the proteolytic site of cleavage (Fig. S4*E*). Assays in *B*, *C*, and *E* were performed in triplicate.

Substrate Cleavage in Cells. Given the high level of Lb^{pro} activity against ISG15 in vitro (Fig. 1 *A* and *B*), we were curious whether this activity and noncanonical cleavage were detectable in a biological context. Transfection of FLAG-tagged ISG15 and the ISG15 assembly machinery (UBE1L, UBE2L6, and HERC5) led to robust ISGylation in HeLa cells. Treatment of these cell lysates with Lb^{pro} collapsed the ISGylated proteins, while free ISG15 remained seemingly unchanged (Fig. 4*A* and Fig. S6*C*). Serendipitously, we observed that ISG15 cross-reacted with a polyclonal antiubiquitin antibody (Fig. S6 *A* and *B*). Treatment with Lb^{pro} specifically removed this cross-reaction, indicating that a fraction of the polyclonal antibody detects an epitope spanning the identical C terminus of both modifiers (Fig. S6 *A* and *B*). Antibody cross-reactivity provided us with a tool to monitor ISG15 cleavage by Lb^{pro} in cell extracts. Indeed, when transfection cell lysates were probed with the polyclonal antiubiquitin antibody, the ISG15 cross-reactive band was no longer detected after Lb^{pro} treatment, indicating that Lb^{pro} had hydrolyzed the ISG15 C terminus (Fig. 4*A*, red box). The antiubiquitin blot also showed that ubiquitin modifications in Lb^{pro}-treated samples were only partially processed, confirming ISG15 preference in complex samples (Fig. 4*A*). This was in stark contrast to the CCHFV vOTU domain, which cleaves ubiquitin and ISG15 similarly (18, 19) and collapsed both types of signals to the same extent (Fig. 4*A*).

To further visualize Lb^{pro} activity, we exploited a previously developed antibody that recognizes GlyGly-modified Lys residues (27, 28). This anti-GlyGly antibody has so far only been used to enrich ubiquitinated tryptic peptides in MS applications (27, 28). Rewardingly, probing these same reactions with the anti-GlyGly antibody produced a smear of strong signals across a wide range of molecular weights in the Lb^{pro}-treated sample (Fig. 4*A*). These signals correspond to the Lb^{pro}-produced GlyGly-modified proteome.

Revealing Lb^{pro} Activity During Viral Infection. To assess the impact of Lb^{pro} activity during viral infection, we first exploited a chimera viral infection model (29). A mengovirus (a strain of encephalomyocarditis, a picornavirus that is closely related to FMDV) system was engineered, in which the Leader protein was inactivated by mutations and functionally replaced by WT Lb^{pro} or catalytically inactive Lb^{pro} Cys51Ala as a leader protease. We monitored Lb^{pro} activity in a time course with anti-ISG15, antiubiquitin, and anti-GlyGly antibodies (Fig. 4*B* and Fig. S6*D*). With inactive Lb^{pro}, ISG15 modifications were visibly increased 6–8 h postinfection, whereas no visible changes to total ubiquitin and no signal in the anti-GlyGly Western blot were apparent. In contrast, mengovirus with active Lb^{pro} resulted in a decrease in ISG15 signals, a slight decrease in ubiquitin signals, and importantly, the appearance of GlyGly-modified proteins at 6 and especially, 8 h postinfection (Fig. 4*B* and Fig. S6*D*). This indicates that, indeed, production of active Lb^{pro} by the virus leads to incomplete hydrolysis of ISG15 and ubiquitin from substrates, which can be visualized using available ubiquitin proteomics antibodies.

Importantly, Lb^{pro} activity can also be visualized during FMDV infection [e.g., using baby hamster kidney (BHK) cells transfected

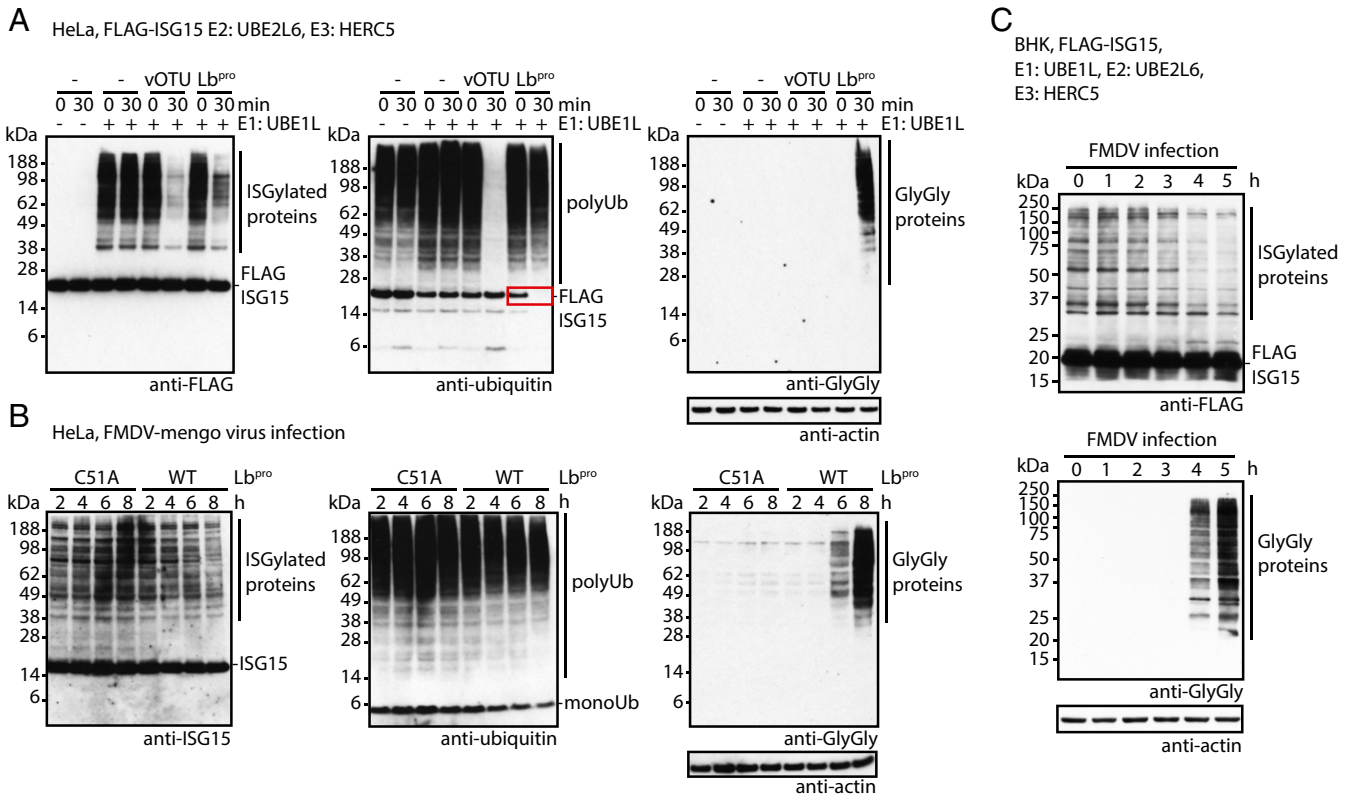

Fig. 4. Validation of Lb^{pro} substrate cleavage in cells. (*A*) Lb^{pro} cleavage assays of ISGylated proteins. HeLa cells were transfected with FLAG-ISG15 and the ISG15 conjugation machinery (UBE1L, UBE2L6, HERC5) to produce ISG15ylated proteins. (*A*, *Left*) Removal of ISG15 from substrates by Lb^{pro} was monitored using an anti-FLAG antibody. (*A*, *Center*) A polyclonal antiubiquitin antibody monitors ubiquitin chain signals but can also be used to monitor cleavage of the ISG15 C terminus by Lb^{pro} (Fig. S6 *A* and *B*) (red box). (*A*, *Right*) The catalytic activity of Lb^{pro} was also monitored using an antibody that recognizes GlyGly-modified Lys residues. Loading controls are in Fig. S6C. (*B*) Infection assays using an FMDV Lb^{pro}-mengovirus chimera. The catalytic activity of Lb^{pro} was monitored as in *A*, with the difference being that ISG15 was detected using an anti-ISG15 antibody (*Left*). A catalytically inactive FMDV Lb^{pro}-mengovirus (C51A) was used as a control. Fig. S6*D* shows loading controls. (*C*) FMDV infection time course using BHK fibroblast cells transfected with FLAG-ISG15 and the ISG15 conjugation machinery. Lb^{pro} catalytic activity was monitored with anti-FLAG (*Top*) and anti-GlyGly (*Bottom*) antibodies. All assays were performed in triplicate.

with FLAG-tagged ISG15 and the ISG15 conjugation system]. Before infection, transfection leads to robust FLAG signals, whereas anti-GlyGly signals are absent. FMDV infection induces collapsing of FLAG signals coinciding with the appearance of GlyGly-modified proteins. Within 4 h of FMDV infection, the anti-GlyGly antibody labels hundreds of proteins across a broad molecular weight range (Fig. 4*C*). We are not aware of a similar host cell-derived viral-induced epitope that is detectable with such relative ease. Importantly, this epitope originates from host proteins and cannot acquire mutations due to viral evolution.

Discussion

Lb^{pro} is a prime example of a viral protein that contributes to successful viral replication through multifunctional roles. In addition to previously known crucial activities during replication (4, 6), we now show how it also hinders antiviral signaling through removal of ISG15 and to a lesser extent, ubiquitin from proteins (Fig. 5). Importantly, its mechanism of incomplete cleavage irreversibly damages the modifiers, which can no longer be attached to proteins. This mechanism is conceptually similar to the activity of RavZ, a *Legionella* effector that hydrolyzes the C terminus of Atg8 ubiquitin-like modifiers involved in autophagy (30). Moreover, on the substrate side, Lb^{pro} activity precludes remodification of Lys residues, and their small GlyGly modification(s) may not alter protein function significantly (Fig. 5). The slight cross-reactivity with ubiquitin is likely important, since ubiquitin modifications are much more abundant, and it is hence difficult to delineate the origin of the observed GlyGly signatures. Nonetheless, these multifaceted traits highlight the importance of Lb^{pro} as a potent virulence factor (31). It is possible that other viruses and pathogens may use this elegant antiinflammatory strategy. While the leader proteases of other picornaviridae are highly divergent on the sequence level, the highly related apthovirus equine rhinitis A virus may also encode an enzyme that generates GlyGly epitopes, which could be tested using GlyGly epitope detection in infected samples.

The here identified virus-induced GlyGly remnants on substrate proteins may lead to improvements in the detection of foot-and-mouth disease (FMD). Vaccination is critical to the control FMD outbreaks; however, it is difficult to distinguish vaccinated from infected animals. Current strategies rely on ELISA-based methods to detect antibodies against nonstructural virus proteins in serum. Our findings suggest that GlyGly-modified proteins could also be used in ELISAs to detect antibodies against this epitope. Detection of antibodies against GlyGly modifications signifies enzymatic activity of Lb^{pro} that would only be observed after viral infection and hence, distinguish infected from vaccinated animals. This utility of detecting FMDV infection may ease the economic burden imposed by FMD, particularly in developing countries, by providing a previously unrecognized biomarker for its detection.

Methods

Cloning and Protein Purification. ISG15 and Met1 diubiquitin were cloned into an His-tagged expression vector (32). The Lb^{pro} vector (23) was expressed and

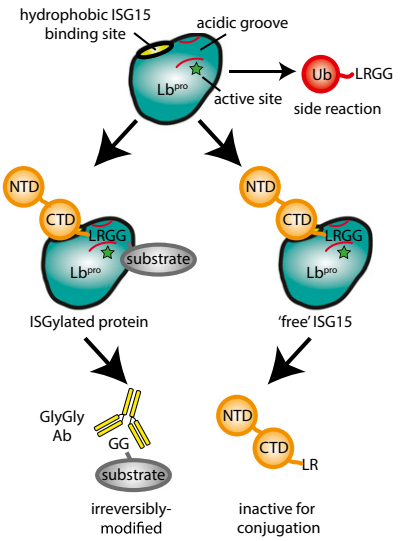

Fig. 5. Model for Lb^{pro} action against ISG15 and ubiquitin. Lb^{pro} preferentially targets ISG15 over ubiquitin, which results from an optimized hydrophobic ISG15 binding site. The acidic groove coordinates the C terminus of ISG15 into the active site of Lb^{pro} and enables cleavage between Arg and GlyGly of the modifiers. This has two consequences: it renders ISG15 or ubiquitin incapable of (re-) conjugation and leaves substrates modified with a GlyGly remnant on their Lys residues. GlyGly-modified Lys remnants can be detected using available antibodies, enabling infection detection strategies. NTD, N-terminal ubiquitin-like domain.

purified according to ref. 33. For the $ISG15^{CTD}$-ΔC probe, ISG15 (amino acids 79–154) was cloned in frame into the intein/chitin binding domain pTXB1 vector. ISG15-intein was expressed and purified according to refs. 17 and 34. *SI Methods* has expression and purifications procedures for His-tagged ISG15 and Met1 diubiquitin.

Biochemistry Assays. ISG15-AMC assays were performed as described previously (18). Ubiquitin/ubiquitin-like TAMRA assays were performed according to ref. 35. ISG15-TAMRA reagent was used to determine Michaelis–Menten kinetics (additional details are in *SI Methods*). Cleavage assays of pro-$ISG15^{CTD}$ and mature $ISG15^{CTD}$ were performed under the same conditions as the TAMRA assays. ISG15 probe assays were also performed under these conditions. *SI Methods* has condition details. MS analysis was performed according to ref. 36.

Crystallography. The Lb^{pro}~$ISG15^{CTD}$-ΔC complex was purified by anion chromatography (Resource Q) and dialyzed into 50 mM Tris, pH 8.0, 50 mM NaCl, 1 mM EDTA, 5 mM DTT, and 5% glycerol. After dialysis, the complex was concentrated to 4 mg/mL and set up at a 1:1 protein:precipitant ratio in a sitting drop vapor diffusion format. Crystals grew in 2.0 M ammonium sulfate, 0.1 M Na citrate, pH 5.6, and 0.2 M K/Na tartrate and were cryoprotected in mother liquor containing 25% glycerol. Crystallographic data were collected at the Diamond Light Source synchrotron (Table S1).

Additional descriptions of the methods are listed in *SI Methods*.

ACKNOWLEDGMENTS. We thank Paul R. Elliott and the beamline scientists at Diamond I-04. Access to Diamond Light Source was supported in part by European Union Seventh Framework Program Infrastructure Grant BIOSTRUCT-X (Contract 283570). This work was supported by The Netherlands Organization for Scientific Research Graduate Program Grant NWO-022.004.018 (to L.J.V.), VICI Grants NWO-724.013.002 (to H.O.) and NWO-918.12.628 (to F.J.M.v.K.) from the Netherlands Organization for Scientific Research, the Biotechnology and Biological Sciences Research Council (Pirbright Institute and T.J.T.), Grants P 24038 (to T.S.) and P 28183 (to T.S.) from the Austrian Science Fund, Medical Research Council Grant U105192732 (to D.K.), European Research Council Grants 309756 (to D.K.) and 724804 (to D.K.), and the Lister Institute for Preventive Medicine (D.K.).

1. Tuthill TJ, Groppelli E, Hogle JM, Rowlands DJ (2010) Picornaviruses. *Curr Top Microbiol Immunol* 343:43–89.
2. Knight-Jones TJD, Rushton J (2013) The economic impacts of foot and mouth disease: What are they, how big are they and where do they occur? *Prev Vet Med* 112: 161–173.
3. Grubman MJ, Baxt B (2004) Foot-and-mouth disease. *Clin Microbiol Rev* 17:465–493.
4. Steinberger J, Skern T (2014) The leader proteinase of foot-and-mouth disease virus: Structure-function relationships in a proteolytic virulence factor. *Biol Chem* 395: 1179–1185.
5. Freimanis GL, et al. (2016) Genomics and outbreaks: Foot and mouth disease. *Rev Sci Tech* 35:175–189.
6. Liu Y, Zhu Z, Zhang M, Zheng H (2015) Multifunctional roles of leader protein of foot-and-mouth disease viruses in suppressing host antiviral responses. *Vet Res* 46:127.
7. Wang D, et al. (2011) The leader proteinase of foot-and-mouth disease virus negatively regulates the type I interferon pathway by acting as a viral deubiquitinase. *J Virol* 85:3758–3766.
8. Isaacson MK, Ploegh HL (2009) Ubiquitination, ubiquitin-like modifiers, and deubiquitination in viral infection. *Cell Host Microbe* 5:559–570.
9. Heaton SM, Borg NA, Dixit VM (2016) Ubiquitin in the activation and attenuation of innate antiviral immunity. *J Exp Med* 213:1–13.
10. Ivashkiv LB, Donlin LT (2014) Regulation of type I interferon responses. *Nat Rev Immunol* 14:36–49.
11. Zhao C, Collins MN, Hsiang T-Y, Krug RM (2013) Interferon-induced ISG15 pathway: An ongoing virus-host battle. *Trends Microbiol* 21:181–186.
12. Durfee LA, Lyon N, Seo K, Huibregtse JM (2010) The ISG15 conjugation system broadly targets newly synthesized proteins: Implications for the antiviral function of ISG15. *Mol Cell* 38:722–732.
13. Zhang X, et al. (2015) Human intracellular ISG15 prevents interferon-α/β over-amplification and auto-inflammation. *Nature* 517:89–93.
14. Bogunovic D, et al. (2012) Mycobacterial disease and impaired IFN-γ immunity in humans with inherited ISG15 deficiency. *Science* 337:1684–1688.
15. Bhoj VG, Chen ZJ (2009) Ubiquitylation in innate and adaptive immunity. *Nature* 458: 430–437.
16. Frias-Staheli N, et al. (2007) Ovarian tumor domain-containing viral proteases evade ubiquitin- and ISG15-dependent innate immune responses. *Cell Host Microbe* 2: 404–416.
17. Pruneda JN, et al. (2016) The molecular basis for ubiquitin and ubiquitin-like specificities in bacterial effector proteases. *Mol Cell* 63:261–276.
18. Akutsu M, Ye Y, Virdee S, Chin JW, Komander D (2011) Molecular basis for ubiquitin and ISG15 cross-reactivity in viral ovarian tumor domains. *Proc Natl Acad Sci USA* 108: 2228–2233.
19. James TW, et al. (2011) Structural basis for the removal of ubiquitin and interferon-stimulated gene 15 by a viral ovarian tumor domain-containing protease. *Proc Natl Acad Sci USA* 108:2222–2227.
20. Basters A, et al. (2014) Molecular characterization of ubiquitin-specific protease 18 reveals substrate specificity for interferon-stimulated gene 15. *FEBS J* 281:1918–1928.
21. van Tilburg GB, Elhebieshy AF, Ovaa H (2016) Synthetic and semi-synthetic strategies to study ubiquitin signaling. *Curr Opin Struct Biol* 38:92–101.
22. Basters A, et al. (2017) Structural basis of the specificity of USP18 toward ISG15. *Nat Struct Mol Biol* 24:270–278.
23. Guarné A, et al. (1998) Structure of the foot-and-mouth disease virus leader protease: A papain-like fold adapted for self-processing and eIF4G recognition. *EMBO J* 17: 7469–7479.
24. Komander D, Clague MJ, Urbé S (2009) Breaking the chains: Structure and function of the deubiquitinases. *Nat Rev Mol Cell Biol* 10:550–563.
25. Deaton MK, et al. (2016) Biochemical and structural insights into the preference of nairoviral deISGylases for interferon-stimulated gene product 15 originating from certain species. *J Virol* 90:8314–8327.
26. Keusekotten K, et al. (2013) OTULIN antagonizes LUBAC signaling by specifically hydrolyzing Met1-linked polyubiquitin. *Cell* 153:1312–1326.
27. Kim W, et al. (2011) Systematic and quantitative assessment of the ubiquitin-modified proteome. *Mol Cell* 44:325–340.
28. Wagner SA, et al. (2011) A proteome-wide, quantitative survey of in vivo ubiquitylation sites reveals widespread regulatory roles. *Mol Cell Proteomics* 10: M111.013284.
29. Rabouw HH, et al. (2016) Middle east respiratory coronavirus accessory protein 4a inhibits PKR-mediated antiviral stress responses. *PLoS Pathog* 12:e1005982.
30. Choy A, et al. (2012) The Legionella effector RavZ inhibits host autophagy through irreversible Atg8 deconjugation. *Science* 338:1072–1076.
31. Chinsangaram J, Mason PW, Grubman MJ (1998) Protection of swine by live and inactivated vaccines prepared from a leader proteinase-deficient serotype A12 foot-and-mouth disease virus. *Vaccine* 16:1516–1522.
32. Berrow NS, et al. (2007) A versatile ligation-independent cloning method suitable for high-throughput expression screening applications. *Nucleic Acids Res* 35:e45.
33. Aumayr M, et al. (2015) NMR analysis of the interaction of picornaviral proteinases Lb and 2A with their substrate eukaryotic initiation factor 4GII. *Protein Sci* 24:1979–1996.
34. Ekkebus R, et al. (2013) On terminal alkynes that can react with active-site cysteine nucleophiles in proteases. *J Am Chem Soc* 135:2867–2870.
35. Geurink PP, El Oualid F, Jonker A, Hameed DS, Ovaa H (2012) A general chemical ligation approach towards isopeptide-linked ubiquitin and ubiquitin-like assay reagents. *ChemBioChem* 13:293–297.
36. Wauer T, et al. (2015) Ubiquitin Ser65 phosphorylation affects ubiquitin structure, chain assembly and hydrolysis. *EMBO J* 34:307–325.